Thermodynamic Properties of an Extremely Rapid Protein Folding Reaction†

Thomas Schindler and Franz X. Schmid*

Laboratorium für Biochemie, Universität Bayreuth, D-95440 Bayreuth, Germany

Received August 20, 1996; Revised Manuscript Received October 8, 1996⊗

ABSTRACT: The cold-shock protein CspB from *Bacillus subtilis* is a very small β-barrel protein, which folds with a time constant of 1 ms (at 25 °C) in a U ⇌ N two-state reaction. To elucidate the energetics of this extremely fast reaction we investigated the folding kinetics of CspB as a function of both temperature and denaturant concentration between 2 and 45 °C and between 1 and 8 M urea. Under all these conditions unfolding and refolding were reversible monoexponential reactions. By using transition state theory, data from 327 kinetic curves were jointly analyzed to determine the thermodynamic activation parameters $\Delta H^{\ddagger}_{H_2O}$, $\Delta S^{\ddagger}_{H_2O}$, $\Delta G^{\ddagger}_{H_2O}$, and $\Delta C^{\ddagger}_{p\,H_2O}$ for unfolding and refolding and their dependences on the urea concentration. 90% of the total change in heat capacity and 96% of the change in the *m* value ($m = d\Delta G/d[\text{urea}]$) occur between the unfolded state and the activated state. This suggests that for CspB the activated state of folding is unusually well structured and almost equivalent to the native protein in its interactions with the solvent. As a consequence of this native-like activated state a strong temperature-dependent enthalpy/entropy compensation is observed for the refolding kinetics, and the barrier to refolding shifts from being largely enthalpic at low temperature to largely entropic at high temperature. This shift originates not from the changes in the folding protein chains itself, but from the changes in the protein−solvent interactions. We speculate that the absence of intermediates and the native-like activated state in the folding of CspB are correlated with the small size and the structural type of this protein. The stabilization of a small β-sheet as in CspB requires extensive non-local interactions, and therefore incomplete sheets are unstable. As a consequence, the critical activated state is reached only very late in folding. The instability of partially folded structure is a means to avoid misfolding prior to the rate-limiting step, and a native-like activated state reduces the risk of non-productive side reactions during the final steps to the native state.

Protein folding reactions vary enormously in rate. Whereas many proteins require minutes or even hours to complete folding (Jaenicke, 1987, 1996), others reach the native state very rapidly, sometimes within a millisecond or less (Jackson & Fersht, 1991b; Khorasanizadeh *et al.*, 1993; Viguera *et al.*, 1994; Sosnick *et al.*, 1994; Huang & Oas, 1995; Kragelund *et al.*, 1995; Schindler *et al.*, 1995). To a first approximation the folding rate of a protein correlates with its size. Small, single-domain proteins with fewer than 100 amino acid residues often fold extremely fast, whereas large proteins with several domains fold much more slowly. The folding of these large proteins is probably a hierarchic process, in which the individual domains first fold very rapidly to an almost native conformation, and then these preformed folding units assemble slowly to the native state (Wetlaufer & Ristow, 1973; Lesk & Rose, 1981; Jaenicke, 1996; Privalov, 1996). Thus, the rate-limiting steps in the folding of small and large proteins are probably different. The folding of large proteins is limited in rate by the need for productive coalescence of the folding domains. This coalescence can be slow because the steric requirements for such a reaction are high and because non-native domain interactions could stabilize off-pathway intermediates. The actual folding reaction, in which the sequence information of a polypeptide chain is read out to assemble the unique native-like conformation, occurs during domain folding and is therefore best studied by using very small single-domain proteins as model systems. From the recent work with small proteins (Huang & Oas, 1995; Kragelund *et al.*, 1995; Schindler *et al.*, 1995, 1996; Khorasanizadeh *et al.*, 1993; Viguera *et al.*, 1994; Sosnick *et al.*, 1996) it is clear that in protein folding the sequence information can be translated into the native threedimensional structure within less than a millisecond and is thus much faster than previously thought.

We are using the cold-shock protein from *Bacillus subtilis*, CspB[1] (Jones *et al.*, 1987; Willimsky *et al.*, 1992), a small protein of 67 residues, to investigate the folding mechanism of an elementary folding unit. The tertiary structure of CspB consists of a single five-stranded β-barrel; α-helices are absent (Figure 1) (Schnuchel *et al.*, 1993; Schindelin *et al.*, 1993). The protein does not contain *cis* prolyl bonds, disulfide bonds, or tightly bound cofactors. Our initial experiments (Schindler *et al.*, 1995) performed at 25 °C showed that CspB folds extremely fast with a time constant of slightly less than a millisecond, and that even in the middle of the urea-induced transition (where folding usually is slowest) the native and the unfolded molecules equilibrate very rapidly with a time constant of 30 ms. Tests for

* To whom correspondence should be addressed. Tel: +49 921 553660. Fax: +49 921 553661. E-mail: franz-xaver.schmid@uni-bayreuth.de.

† This work was supported by grants from the Deutsche Forschungsgemeinschaft and the Fonds der Chemischen Industrie.

⊗ Abstract published in *Advance ACS Abstracts,* December 1, 1996.

[1] Abbreviations: CspB, cold-shock protein; λ, measured rate constant of a chemical reaction; k_{ij}, microscopic rate constant. Thermodynamic parameters, extrapolated to 0 M urea, are denoted by the subscript H_2O, their dependences on the urea concentration ($d\Delta X/d[\text{urea}]$) by the subscript *i*, and activation parameters by the superscript "‡".

S0006-2960(96)02090-9 CCC: $12.00

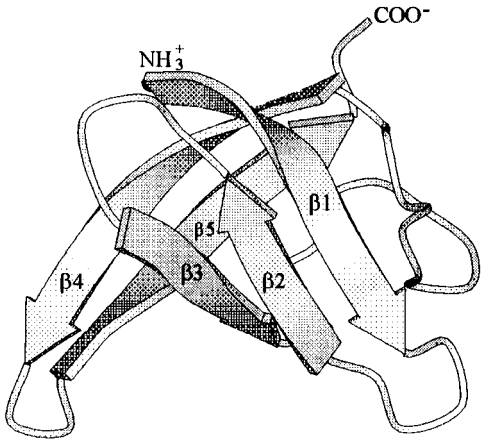

FIGURE 1: Ribbon drawing of the cold-shock protein CspB from *B. subtilis*. The tertiary structure of CspB consists of a single five-stranded β-barrel. This MOLSCRIPT (Kraulis, 1991) representation is based on the coordinates of Schindelin *et al.* (1993).

partially-folded intermediates were negative both in the equilibrium transition and in the folding kinetics.

To understand the energetics of such an elementary folding reaction, we have now investigated the folding kinetics of CspB as a function of the urea concentration at 14 different temperatures between 2 and 45 °C. Under all these conditions folding follows a two-state mechanism and therefore these extensive data could be used for a joint analysis to determine the activation parameters $\Delta G^{\ddagger}_{H_2O}$, $\Delta H^{\ddagger}_{H_2O}$, $\Delta S^{\ddagger}_{H_2O}$, and $\Delta C^{\ddagger}_{p,H_2O}$ for unfolding and refolding. The differences of these activation parameters are consistent with the equilibrium thermodynamic parameters under all experimental conditions. This analysis shows that the activated state of this fast folding reaction of a small β-sheet protein is native-like.

MATERIALS AND METHODS

Materials. Urea (ultrapure) was from ICN (Cleveland, OH, U.S.A.). All other chemicals were from Merck (Darmstadt, Germany). The concentration of urea was determined by the refraction of the solution according to Pace *et al.* (1986). CspB from *B. subtilis* was overexpressed in *Escherichia coli* using the bacteriophage T7 RNA polymerase promotor system (Schindelin *et al.*, 1992) and purified as described previously (Schindler *et al.*, 1995).

Stopped-Flow Kinetic Experiments. A DX.17MV sequential mixing stopped-flow spectrometer from Applied Photophysics (Leatherhead, U.K.) was used for all kinetic measurements. The path length of the observation chamber was 2 mm, and a 10 mM aqueous solution of cytidine-2′-phosphate in a 0.2 cm cell was inserted between the observation chamber and the emission photomultiplier to absorb scattered light from the excitation beam. The folding kinetics were followed by the change in fluorescence above 300 nm after excitation at 280 nm (10 nm bandwidth). The zero time point and the dead time of mixing of the stopped-flow instrument under our experimental conditions were determined by using the reaction between 2,6-dichlorophenolindophenol and L-ascorbate and the procedure suggested by Tonomura *et al.* (1978). The dead time of mixing was about 1.2 ms, and reactions with rate constants smaller than 800 s^{-1} could be followed in the single-mixing experiments.

All unfolding and refolding experiments were carried out in 0.1 M sodium cacodylate/HCl pH 7.0. To initiate unfolding typically 12 μM native CspB in buffer was diluted 6-fold with urea solutions of varying concentrations to give final urea concentrations between 2 and 8 M (depending on temperature). To initiate refolding 12 μM unfolded CspB in high-molar urea (between 5 and 8 M, depending on temperature) was diluted 6-fold with aqueous buffer or with urea solutions of varying concentrations to give final concentrations of 1−4 M urea. Kinetics were measured at least eight times under identical conditions, averaged, and analyzed as monoexponential functions by using the software provided by Applied Photophysics.

Analysis of the Folding Kinetics. For a two-state folding reaction as in eq 1 the measured rate constant λ is equal to the sum of the microscopic rate constants for refolding (k_{UN}) and unfolding (k_{NU}) (eq 2).

$$N \underset{k_{UN}}{\overset{k_{NU}}{\rightleftharpoons}} U \tag{1}$$

$$\lambda = k_{NU} + k_{UN} \tag{2}$$

The transition state theory relates an individual reaction rate constant with the Gibbs free energy of the activated state relative to the initial state $\Delta G^{\ddagger}$ (eq 3).

$$k_{ij} = \frac{k_B T}{h} \exp\left(\frac{-\Delta G^{\ddagger}(T)}{RT}\right) \tag{3}$$

In eq 3 k_B, h, and R are the Boltzmann, the Planck, and the universal gas constants, respectively. In analogy to the equilibrium Gibbs free energy ΔG, the activation Gibbs free energy $\Delta G^{\ddagger}$ can be decomposed into its (temperature-dependent) enthalpic and entropic components as shown in eq 4. Thus $\Delta H^{\ddagger}$ is the enthalpy of activation, $\Delta S^{\ddagger}$ the entropy of activation, and $\Delta C^{\ddagger}_p$ the change in heat capacity going from the initial to the activated state at the reference temperature $T°$, which is 298.15 K (25 °C) in our calculations. $\Delta C^{\ddagger}_p$ is assumed not to depend on temperature in this narrow temperature range (2−45 °C).

$$\Delta G^{\ddagger}(T) = \Delta H^{\ddagger}(T°) - T\Delta S^{\ddagger}(T°) + \Delta C^{\ddagger}_p\left[(T - T°) - T\ln\left(\frac{T}{T°}\right)\right] \tag{4}$$

As the equilibrium thermodynamic parameters, the activation parameters are assumed to vary linearly with the denaturant concentration (5a−c).

$$\Delta H^{\ddagger}(T°) = \Delta H^{\ddagger}_{H_2O}(T°) + \Delta H^{\ddagger}_i(T°)[\text{urea}] \tag{5a}$$

$$\Delta S^{\ddagger}(T°) = \Delta S^{\ddagger}_{H_2O}(T°) + \Delta S^{\ddagger}_i(T°)[\text{urea}] \tag{5b}$$

$$\Delta C^{\ddagger}_p = \Delta C^{\ddagger}_{p,H_2O} + \Delta C^{\ddagger}_{p,i}[\text{urea}] \tag{5c}$$

In eqs 5a−c $\Delta H^{\ddagger}_{H_2O}$, $\Delta S^{\ddagger}_{H_2O}$, and $\Delta C^{\ddagger}_{p,H_2O}$ are the enthalpy, entropy, and heat capacity of activation in the absence of denaturant at $T = T°$ (298.15 K) and $\Delta H^{\ddagger}_i$, $\Delta S^{\ddagger}_i$, and $\Delta C^{\ddagger}_{p,i}$ describe their respective dependence on the denaturant concentration at $T°$. Combination of the eqs 3, 4, and 5a−c leads to two equations as in eq 6 which take into

$$k_{ij} = \left(\frac{k_B T}{h}\right)\left[\left(\frac{T}{T^\circ}\right)(\Delta C^{\ddagger}_{p,H_2O} + \Delta C^{\ddagger}_{p,i}[\text{urea}])/R\right] \exp[(\Delta S^{\ddagger}_{H_2O}(T^\circ) + \Delta S^{\ddagger}_{i}(T^\circ)[\text{urea}])/R - (\Delta H^{\ddagger}_{H_2O}(T^\circ) + \Delta H^{\ddagger}_{i}(T^\circ)[\text{urea}])/RT - (\Delta C^{\ddagger}_{p,H_2O} + \Delta C^{\ddagger}_{p,i}[\text{urea}])(T - T^\circ)/\text{RT}] \quad (6)$$

account the dependences on temperature and urea concentration of the microscopic rate constants of unfolding and refolding, k_{NU} and k_{UN}. These two equations contain the activation parameters of the unfolding and the refolding reaction, respectively. They were then combined as in eq 2 to describe the dependences on temperature and urea concentration of the measured rate constant λ. For the joint nonlinear least-squares fit of all measured values of λ to the combined eq 2 and 6 the program Grafit 3.0 (Erithacus Software, Staines, U.K.) was used.

Heat-Induced Equilibrium Unfolding Transitions. Thermal denaturation curves at different urea concentration were recorded with a Hewlett-Packard 8452A diode array spectrometer equipped with a Peltier element and the temperature was measured with a sensor which was directly inserted into the cell. The accuracy of the temperature sensor was checked by using a calibrated precision thermometer (Brand, Wertheim, Germany). The protein concentration was typically 120 μM in 1 cm cells, and the buffer was 0.1 M sodium cacodylate/HCl, pH 7.0. The samples were heated at a rate of 0.6 °C per minute. Unfolding was monitored by the decrease in absorbance at 292 nm relative to 314 nm, where the protein does not absorb. The reversibility was examined by subsequent cooling of the samples to the starting temperature. The absorbance values were divided by the protein concentration to obtain the molar absorbance ϵ_{292}. The transition curves were analyzed by a nonlinear least-squares fit of ϵ_{292} as a function of temperature and urea concentration to eq 7 using the program Grafit 3.0 (Erithacus Software, Staines, U.K.). Equation 7 relates the change in absorption y with the temperature and urea concentration to the thermodynamics of a two-state unfolding reaction.

$$y(T,[\text{urea}]) = y_N - \frac{y_N - y_U}{1 + \exp\{\Delta G(T)/RT\}} \quad (7a)$$

with

$$\Delta G(T) = \Delta H_{H_2O}(T^\circ) + \Delta H_i(T^\circ)[\text{urea}] - T(\Delta S_{H_2O}(T^\circ) + \Delta S_i(T^\circ)[\text{urea}]) + (\Delta C_{p,H_2O} + \Delta C_{p,i}[\text{urea}])\left[(T - T^\circ) - T\ln\left(\frac{T}{T^\circ}\right)\right] \quad (7b)$$

$$y_N = y_N^0 + m_N[\text{urea}] + n_N T + q_N[\text{urea}]T \quad (7c)$$

$$y_U = y_U^0 + m_U[\text{urea}] + n_U T + q_U[\text{urea}]T \quad (7d)$$

In eq 7b ΔH_{H_2O}, ΔS_{H_2O}, and $\Delta C_{p,H_2O}$ are the enthalpy, entropy, and heat capacity of protein unfolding in the absence of denaturant at T° = 298.15 K and ΔH_i, ΔS_i, and $\Delta C_{p,i}$ describe their respective dependence on the denaturant concentration at T°. The absorbances of the native protein (y_N) and of the unfolded protein (y_U) are assumed to depend linearly on both "denaturing parameters", i.e., temperature and urea concentration. The values of y_N^0 and y_U^0 are those at T = 0 K and [urea] = 0 M, and m_N, m_U, n_N, and n_U define the dependences of y_N and y_U on temperature and on urea concentration, respectively. We included the additional parameters q_N and q_U into eq 7 to account for the possibility that the slopes of the base lines in thermal transitions can vary with the urea concentration, or in other words that the dependences of y_N and y_U on temperature and on urea concentration are not necessarily independent. The fit parameters were almost unchanged when q_N and q_U in eq 7 were set to 0, but the quality of the fit was slightly less satisfactory.

RESULTS

Unfolding and Refolding Kinetics As a Function of Urea Concentration and Temperature. The folding kinetics of CspB were followed by the fluorescence of Trp8, which is partially buried in the native state (Schnuchel *et al.*, 1993; Schindelin *et al.*, 1993). Its emission decreases about 2-fold upon unfolding (Schindler *et al.*, 1995). Unfolding and refolding were typically initiated by a 6-fold stopped-flow dilution of the native and the unfolded protein, respectively, to the desired final conditions. Folding was reversible in the entire range of temperature (2−45 °C) and urea concentration (1−8 M). Under all of these conditions unfolding and refolding followed single exponential time courses, and the observed amplitudes accounted for the entire change in fluorescence. As observed previously at 25 °C (Schindler *et al.*, 1995), the initial values of the unfolding kinetics followed the extrapolated base line of the native protein, and those of the refolding kinetics followed the extrapolated base line of the unfolded protein. In all cases where unfolding and refolding kinetics were measured under the same final conditions, identical apparent rate constants (λ) and final values were obtained, as expected for a reversible reaction. Since CspB is a very small protein, the cooperativity of the urea-induced unfolding transition is low and overlapping unfolding and refolding kinetics could be measured over a broad range of urea concentrations. These favorable properties of the folding reaction of CspB together with its excellent reversibility enabled us to measure and analyze its kinetics solely on the basis of the kinetic data without the need to extrapolate unfolding data over several concentration units of urea or to include stability data into the analysis. Instead, the comparison of the kinetic and equilibrium data could be used to test the validity of the two-state model.

The unfolding and refolding kinetics of CspB were determined between 1 and 8 M urea at 14 different temperatures between 2 and 45 °C. In Figure 2 the measured rate constants λ are shown as a function of the urea concentration for nine of these temperatures. The visual inspection of the kinetic data in Figure 2 reveals that the folding of CspB is fast in the entire temperature range. The slowest rate (λ = 3 s^{-1}) was found for the equilibration between native and unfolded CspB in the middle of the transition at 2 °C, but under these conditions N ⇌ U equilibration is still complete within about 1 s.

As observed for most other proteins, the measured rate constants λ of folding follow a V-shaped dependence on denaturant concentration (Tanford, 1968; Matthews, 1993) for CspB as well. At all temperatures, however, this V-shape is strongly asymmetric. The unfolding limb is fairly flat

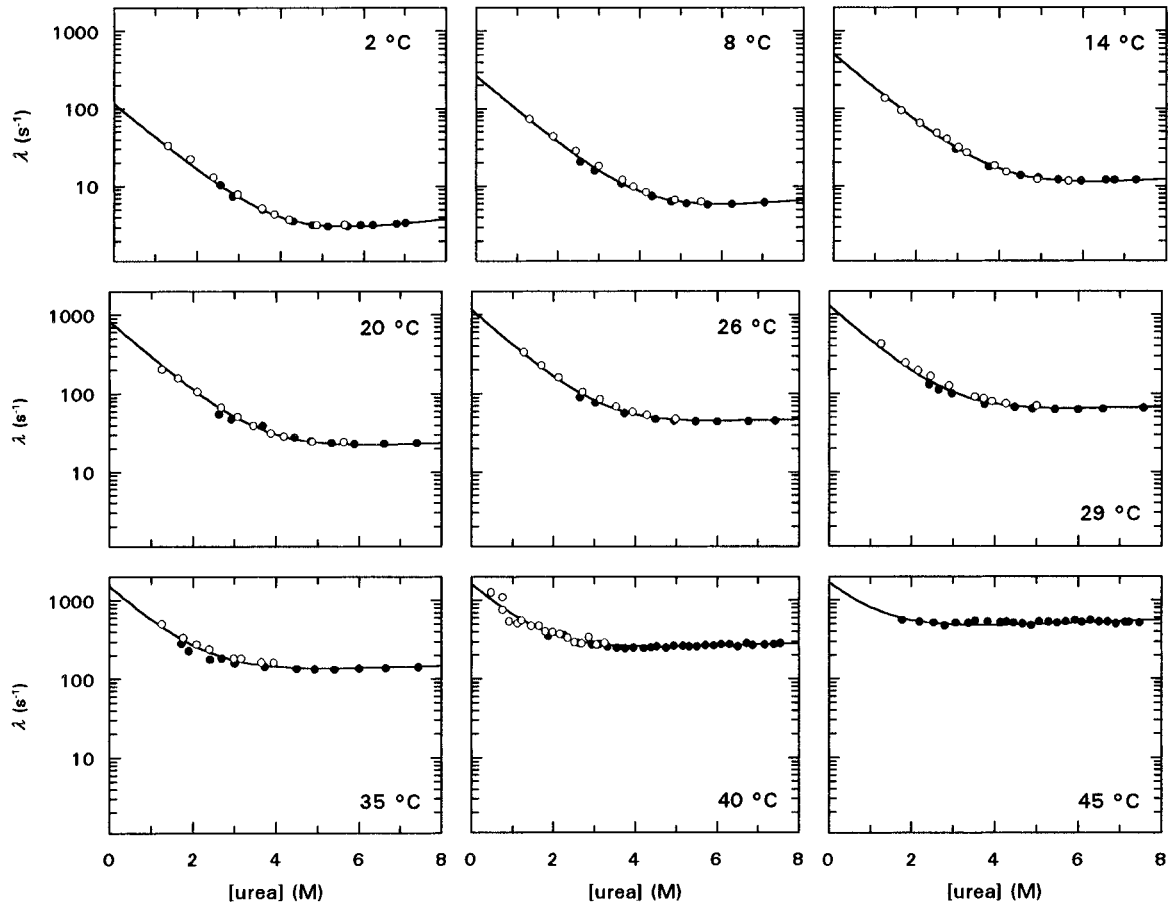

FIGURE 2: Dependence of the apparent rate constant λ of unfolding (●) and refolding (○) of CspB on the urea concentration at different temperatures. A total of 327 data points (at 14 different temperatures) were subjected to a joint fit to combined eqs 2 and 6. The profiles for λ as calculated from the fit parameters in Table 1 are shown by the solid lines for each temperature. The kinetics were monitored by the change in fluorescence above 300 nm in 0.1 M sodium cacodylate/HCl, pH 7.0.

because the rate of unfolding of CspB is almost independent of the urea concentration. This is most clearly seen for the kinetics measured at 45 °C (Figure 2). At this high temperature the protein is only marginally stable, and the measured rate of unfolding is practically independent of the urea concentration between 2 and 8 M.

At a constant urea concentration (e.g., at 7 M) the rate constant of unfolding increases steadily with temperature from about 4 s^{-1} at 2 °C to about 500 s^{-1} at 45 °C. The rate constant of refolding, as measured at 1 M urea shows a complex dependence on temperature. From 40 s^{-1} at 2 °C it increases significantly to values near 500 s^{-1} at 25 °C and remains in this range when the temperature is further increased. This shows that the apparent Arrhenius activation energy of refolding is not constant, but decreases with temperature, either because the mechanism of refolding changes or, more likely, because the heat capacity of the system decreases during refolding.

Analysis of the Folding Kinetics. We could not find evidence for folding intermediates in this and in previous work, and therefore we used the simple two-state model of eq 1 for analyzing the observed kinetics. For a two-state reaction the measured rate constant λ is equal to the sum of the microscopic rate constants of unfolding and refolding k_{NU} and k_{UN} (eq 2). The folding of CspB follow monoexponential time courses under all our conditions, and kinetics with identical rate constants (but opposite amplitudes) were observed for unfolding and refolding under the same final conditions. Together, this suggests that the principle of microscopic reversibility holds and that the protein uses the same transition state (or a set of energetically similar transition states) in unfolding and refolding. Therefore, as proposed by other investigators (Tanford, 1968; Matouschek *et al.*, 1990; Chen & Matthews, 1994; Creighton *et al.*, 1996), we used transition state theory to analyze the folding kinetics and assumed that similar to the equilibrium thermodynamic parameters (Schellman, 1978; Pace, 1986; Agashe & Udgaonkar, 1995; Schindler *et al.*, 1995) the activation parameters for unfolding and for refolding depend linearly on the concentration of the denaturant.

As shown in the Materials and Methods section, we combined the Eyring equations for k_{NU} and k_{UN} (eq 6) to express the measured rate constant λ as a function of the urea concentration and the temperature. This relation was used for a joint fit of the entire data set, which consisted of 327 values for λ measured between 1 and 8 M urea at 14 different temperatures. 12 parameters were obtained from this fit: the activation enthalpies $\Delta H^{\ddagger}_{H_2O}$, activation entropies $\Delta S^{\ddagger}_{H_2O}$, and activation heat capacities $\Delta C^{\ddagger}_{p,H_2O}$, of unfolding and of refolding and the dependences of these parameters on the urea concentration, $\Delta X^{\ddagger}_i = d\Delta X^{\ddagger}/d[\text{urea}]$. They are given in Table 1. To complete the data set $\Delta G^{\ddagger}$ and $\Delta G^{\ddagger}_i$ were calculated from the activation enthalpies and entropies. They are also listed in Table 1. Note that $\Delta G^{\ddagger}_i$ describes the dependence of $\Delta G^{\ddagger}$ on urea concentration and is thus identical with the kinetic *m* value (with *m* being defined as $-RT$ d ln k_{ij}/d[urea]).

Table 1: Activation Parameters of the Folding Reaction of CspB at pH 7.0, 25 °C[a]

	U ⇀ TS	N ⇀ TS	N ⇌ U[b]
ΔH_{H_2O} (kJ/mol)	31.6 ± 2.2	96.1 ± 3.3	64.4 ± 4.0
ΔH_i [kJ/(mol·M)]	−2.38 ± 1.55	−1.28 ± 0.53	1.1 ± 1.6
ΔS_{H_2O} [J/(mol·K)]	−81 ± 7	106 ± 11	186 ± 13
ΔS_i [J/(mol·K·M)]	−17 ± 5	−3.9 ± 1.8	13 ± 6
$\Delta C_{p,H_2O}$ [kJ/(mol·K)]	−2.7 ± 0.3	0.3 ± 0.4	3.0 ± 0.5
$\Delta C_{p,i}$ (J/(mol·K·M))	−66 ± 135	149 ± 70	216 ± 152
ΔG_{H_2O} (kJ/mol)	55.7[c]	64.6[c]	8.9[c]
ΔG_i [kJ/(mol·M)]	−2.67[c]	0.10[c]	2.77[c]

[a] The activation parameters result from the joint fit of a set of 327 rate constants (measured over a temperature range from 2 to 45 °C and a urea concentration range of 1−8 M) according to eqs 2 and 6. All measurements were carried out in 0.1 M sodium cacodylate/HCl, pH 7.0. ΔX_{H_2O}, thermodynamic parameter in the absence of urea; ΔX_i, urea dependence of the respective thermodynamic parameter [X standing either for H (reaction enthalpy), S (reaction entropy), C_p (heat capacity), or G (Gibbs free energy)]. [b] Difference between the activation parameters of unfolding and refolding. [c] Standard deviations are not given for ΔG_{H_2O} and ΔG_i because these parameters do not result from the fits to eqs 2 and 6. The errors in ΔG_{H_2O} and ΔG_i can be obtained at the individual temperatures by fitting the kinetic data to eqs 2 and 3 and by assuming that the $\Delta G^{\ddagger}$ values depend linearly on the concentration of urea. From these fits we obtain standard deviations of ±1.0 kJ/mol for the $\Delta G^{\ddagger}$ values and of ±0.25 kJ/(K·mol) for the ΔG_i values.

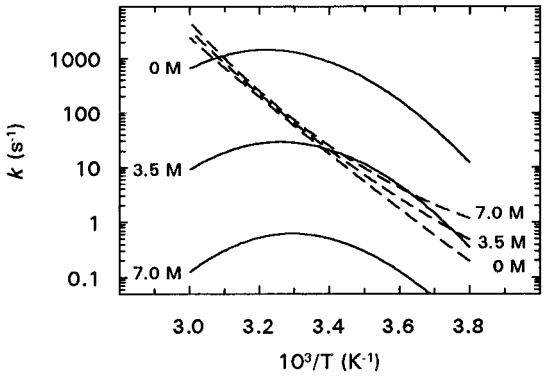

FIGURE 3: Arrhenius plot of the microscopic rate constant k of unfolding (dashed lines) and refolding (solid lines) of CspB at 0, 3.5, and 7 M urea, as indicated. The lines were calculated from the parameters given in Table 1 (cf. legend to Figure 2).

The activation parameters from this joint fit and eqs 2 and 6 were then used to calculate λ as a function of the urea concentration at the individual temperatures. These calculated profiles are shown by the continuous lines in Figure 2. They follow the experimental λ values very well at all urea concentrations and at all temperatures. No systematic deviations are found, which provides initial evidence that the simple two-state model and the extension of the linear free energy relationship to the activation parameters indeed describes the measured folding kinetics very well under all our experimental conditions. It should be noted that a nonlinear dependence of the activation free energy of unfolding on the denaturant concentration was found for barnase, chymotrypsin inhibitor (Matouschek *et al.*, 1995), and Arc repressor (Jonsson *et al.*, 1996), in both cases at very high denaturant concentrations.

The activation parameters in Table 1 were also used to calculate the microscopic rate constants of unfolding and refolding, k_{NU} and k_{UN}, as a function of temperature under three different conditions: in the native base line region (at 0 M urea), in the transition region (at 3.5 M urea), and in the unfolded base line region (at 7 M urea). The respective

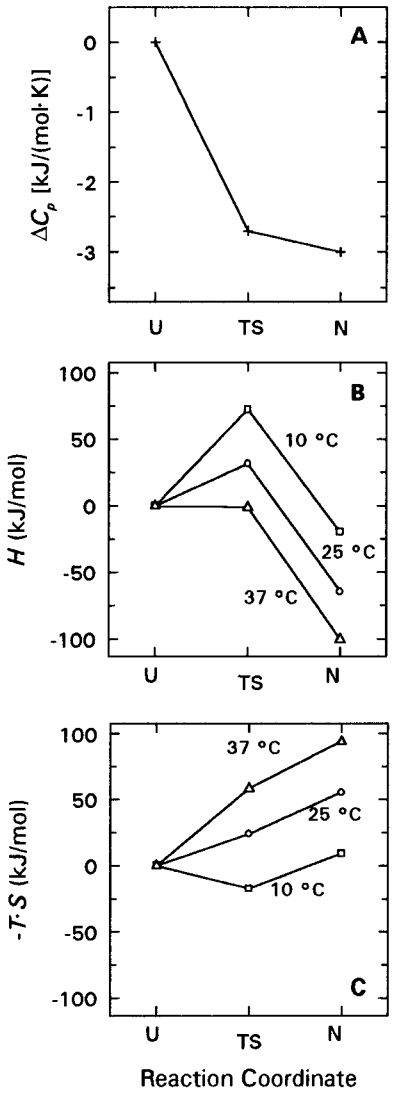

FIGURE 4: Reaction profiles for the folding of CspB at pH 7.0, 0 M urea when going from the unfolded state (U) via the transition state (TS) to the native state (N). The heat capacity (panel A) is assumed not to depend on temperature in the range studied. The enthalpy H (panel B) and the corresponding entropic term $-TS$ (panel C) are shown for 10 °C (□), 25 °C (○), and 37 °C (△) and refer to the fit results given in Table 1. The traces in B and C are arbitrarily aligned such that the values for U coincide.

Arrhenius plots are shown in Figure 3. The three traces for ln k_{NU} almost coincide, because the rate constant of unfolding is barely dependent on the urea concentration (cf. also Figure 2). Furthermore, ln k_{NU} depends almost linearly on $1/T$ at the three denaturant concentrations.

A different behavior is found for the rate constant of refolding k_{UN}. The three profiles for ln k_{UN} are curved with maxima at 37 °C (0 M urea), 34 °C (3.5 M urea), and 30 °C (7.0 M urea). Though similar in shape, the profiles for k_{UN} are strongly displaced along the k axis in Figure 3 because k_{UN} decreases strongly with increasing urea concentration.

The differences in the temperature profiles for ln k_{NU} and ln k_{UN} in Figure 3 are a consequence of the strongly different activation heat capacities of unfolding and refolding (Table 1). The absolute value of $\Delta C^{\ddagger}_{p\,H_2O}$ is 10-fold higher in refolding than in unfolding. This implies that in the refolding direction 90% of the change in ΔC_p has already occurrred when the activated state is reached (Figure 4A), or, in other words, the activated state of folding is about "90% native"

by this criterion. The $\Delta C_p^{\ddagger}$ values of unfolding and refolding show different dependences on urea concentrations (cf. the $C_{p,i}^{\ddagger}$ values in Table 1 and the slight increase in the curvature of the profile for ln k_{NU} with urea concentration in Figure 3) and therefore at 6 M urea the activated state is only "70% native" as judged by $\Delta C_p^{\ddagger}$.

Ln k_{NU} and ln k_{UN} depend differently also on the urea concentration. For unfolding the Gibbs free energy of activation, $\Delta G^{\ddagger}$, is almost independent of the denaturant concentration and $\Delta G_i^{\ddagger}$(N→U) is extremely small [0.1 kJ/(mol·M), Table 1]. In contrast, for refolding $\Delta G_i^{\ddagger}$ is large and negative [$\Delta G_i^{\ddagger}$(U→N) = −2.67 kJ/(mol·M), Table 1]. $\Delta G_i^{\ddagger}$ is equivalent with the kinetic *m* value, and the very small value for $\Delta G_i^{\ddagger}$(N→U) suggests that the native state and the activated state of folding are almost identical in their interaction with the denaturant. As a consequence of the very small value for $\Delta G_i^{\ddagger}$(N→U) the unfolding limbs of the V-shaped kinetic profiles in Figure 2 are almost flat and the Arrhenius profiles for the unfolding rate constant k_{NU} at different urea concentrations almost coincide (cf. Figure 3).

The enthalpic (ΔH) and entropic ($T\Delta S$) contributions to the Gibbs free energy (ΔG) are shown in Figure 4B,C as a function of the reaction coordinate at three different temperatures. For this comparison the values of the unfolded protein (U) were set to zero. The activation heat capacity of refolding is large and that of unfolding is very small (cf. Table 1), and therefore $\Delta H^{\ddagger}$ and $T\Delta S^{\ddagger}$ vary strongly with temperature in refolding (U→N) but not in unfolding (N→U). At 25 °C $\Delta H^{\ddagger}$ of unfolding (N→ U) is large and positive (96 kJ/mol) and $T\Delta S^{\ddagger}$ is also positive (30 kJ/mol). This large value of $\Delta H^{\ddagger}$ shows that there is an enthalpic barrier to unfolding for CspB. The positive activation entropy would favor the formation of the transition state from the native state. Since the $\Delta C_p^{\ddagger}$ value for unfolding is almost zero this scenario does not change significantly between 10 and 37 °C. At all temperatures $\Delta H^{\ddagger}$(N→U) remains large and positive and is counteracted by a large $T\Delta S^{\ddagger}$ value (Figure 4B,C).

For refolding (U→N) at 25 °C $\Delta H^{\ddagger}$ is also positive (32 kJ/mol), but $T\Delta S^{\ddagger}$ is negative (−24 kJ/mol), suggesting that in refolding CspB encounters an enthalpic as well as an entropic barrier. However, the $\Delta C_p^{\ddagger}$ value of refolding is very large, and thus both $\Delta H^{\ddagger}$(U→N) and $T\Delta S^{\ddagger}$(U→N) depend strongly on temperature. Therefore we observe a strong enthalpy/entropy compensation in the activation parameters of refolding. At 10 °C a small positive $T\Delta S^{\ddagger}$ value is overcompensated by a large positive $\Delta H^{\ddagger}$ value pointing to a purely enthalpic barrier to folding at low temperature (Figure 4B,C). $\Delta H^{\ddagger}$ decreases strongly with temperature, and at 37 °C, $\Delta H^{\ddagger}$ is close to zero whereas $T\Delta S^{\ddagger}$ is strongly negative. Thus the barrier to refolding seems to be entirely entropic at high temperature.

This interpretation has to remain tentative as far as $\Delta S^{\ddagger}$ is concerned, because the activation entropies depend on the pre-exponential factor in the Eyring equation. Therefore the absolute values for $T\Delta S^{\ddagger}$ (and also for $\Delta G^{\ddagger}$) in Table 1 and Figure 4 are not known. Still, the changes in $T\Delta S^{\ddagger}$ with temperature are independent of its absolute value, and the observed compensation between the enthalpy and the entropy of activation as well as the resulting change in the nature of the activation barrier (being largely enthalpic at low and largely entropic at high temperature) remain to be major properties of the refolding reaction of CspB.

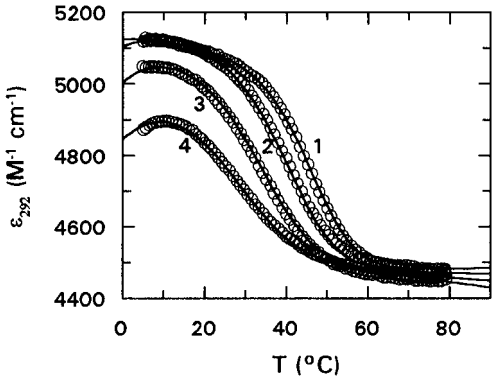

FIGURE 5: Heat-induced equilibrium unfolding transitions of CspB in 0.1 M sodium cacodylate/HCl pH 7.0 in the presence of (1) 1 M, (2) 2 M, (3) 3 M, and (4) 4 M urea. The transitions were monitored by the decrease in absorbance at 292 nm (ϵ_{292}). The unfolding curves were subjected to a joint fit on the basis of the two-state model according to eq 7. The best fit curves are shown by the continuous lines through the data. The thermodynamic parameters from the joint fit are given in Table 2.

Consistency between the Kinetic Activation Parameters and the Equilibrium Stability of CspB. For a two-state reaction as in eq 1 the differences between the activation parameters of the forward and the reverse reactions should be equal to the equilibrium thermodynamic parameters (eq 8). Accordingly, for the unfolding of CspB ΔH(eq), ΔS(eq), ΔG(eq), and ΔC_p(eq) as well as their dependences on the urea concentration were calculated from the activation parameters. They are shown in the last column of Table 1.

$$\Delta X(\text{eq}) = \Delta X^{\ddagger}(\text{U}\rightarrow\text{N}) - \Delta X^{\ddagger}(\text{N}\rightarrow\text{U}) \qquad (8)$$

To investigate whether these differences between the activation parameters are consistent with the equilibrium thermodynamic parameters we measured in independent experiments the equilibrium unfolding transition of CspB by the decrease in tryptophan absorbance at 292 nm as a function of the temperature at 0, 1, 2, 3, and 4 M urea. In the absence of urea the thermal unfolding of CspB was only 90% reversible, because the protein aggregated slightly above 70 °C. At 1−4 M urea the transitions were reversible; they are shown in Figure 5. Because of the low stability of CspB the base line of the native protein (at low temperature) is reached only in the presence of ≤1 M urea. At >1 M urea cold denaturation occurs below about 10 °C and the stability curves show maxima near this temperature.

Similar to the kinetic data the equilibrium transitions in Figure 5 were subjected to a joint fit based on the two-state mechanism in eq 1. Equation 7 in the Methods section describes the dependence of ϵ_{292} on urea concentration and temperature. As in the analysis of the kinetic data we assumed that all equilibrium transitions are described by a single set of thermodynamic parameters ΔH(eq), ΔS(eq), and ΔC_p(eq), and their linear dependences on the concentration of urea [ΔH_i(eq), ΔS_i(eq), and $\Delta C_{p,i}$(eq)]. Equation 7 was used to analyze the experimental data in Figure 5, and the parameters at 25 °C and 0 M urea, resulting from the joint fit of the thermal unfolding curves in Figure 5 are given in the first column of Table 2. They agree well with the parameters that were calculated from the difference of the activation parameters (as shown in the second column of Table 2).

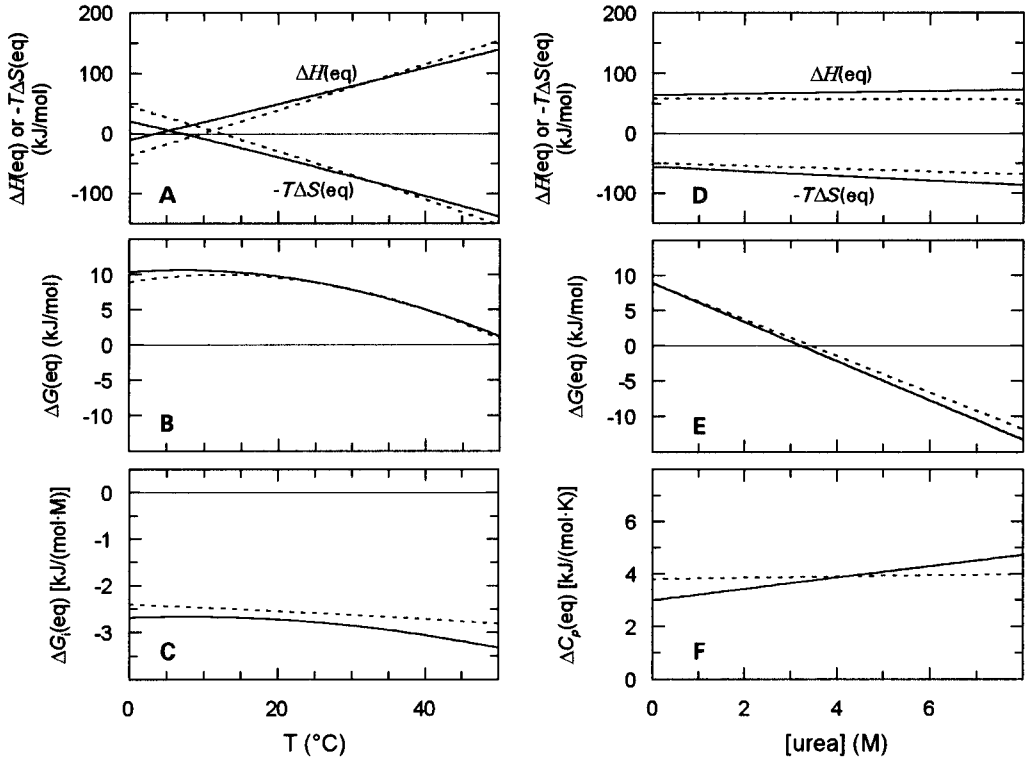

FIGURE 6: Comparison of the thermodynamic parameters of unfolding of CspB in 0.1 M sodium cacodylate/HCl, pH 7.0, obtained from the kinetic experiments (solid lines) and from thermal unfolding (broken lines). The enthalpy ΔH(eq), the entropy, given as $-T\Delta S$(eq), and the Gibbs free energy ΔG(eq) of unfolding in the absence of urea are plotted as a function of the temperature in panels A and B. In panel C the dependence of the Gibbs free energy of unfolding on the denaturant ΔG_i(eq) is shown as a function of temperature. It is identical with the classical *m*-value. In panels D−F the enthalpy ΔH(eq), the entropy, given as $-T\Delta S$(eq), the Gibbs free energy ΔG(eq) of unfolding, and the heat capacity change ΔC_p(eq) upon unfolding are given as a function of the urea concentration at the reference temperature of 25 °C.

To provide a deeper insight into the consistency between the equilibrium and the kinetic data we cut two orthogonal slices through the fitted data and compared them as a function of temperature at 0 M urea (Figure 6A−C) and as a function of the urea concentration at 25 °C (Figure 6D−F). The values for the Gibbs free energy of denaturation ΔG(eq) (Figure 6B,E) from the equilibrium and the kinetic experiments coincide very well over the entire range of temperature and urea concentrations. Also, its dependence on urea concentration (the ΔG_i or *m* values in Figure 6C) agree within about 10% over the entire temperature range. The individual components ΔH(eq) and $T\Delta S$(eq) are also very similar, although their dependences on temperature are slightly different (Figure 6A).

A marked difference is found only for ΔC_p (Figure 6F). At 0 M urea the value from the kinetics [3.0 kJ/(K·mol)] is smaller than the equilibrium value of 3.8 kJ/(K·mol) and also smaller than the calorimetric value of 3.7 kJ/(K·mol) (Makhatadze & Marahiel, 1994). This difference is responsible for the variations in the slopes of ΔH(eq) and TΔS(eq) in Figure 6A. The ΔC_p(eq) value from the kinetics increases more strongly with urea and the two lines for ΔC_p(eq) in Figure 6F intersect near 4 M urea. ΔC_p is the second derivative of the measured values K_{eq} and k_{ij} and therefore (together with the *m* values) shows the highest uncertainty. We therefore doubt, whether the differences in ΔC_p(eq) and its dependence on the urea concentration have a real physical background. Rather, they could be a consequence of compensating changes that originate from the data fitting.

It should be noted that in general the values for ΔH_i, ΔS_i, and $\Delta C_{p,i}$ are small and show a high relative error. Therefore it remains unclear whether the activation enthalpies, entropies, and heat capacities in Table 1 depend on the denaturant concentration. ΔH_i, ΔS_i, and $\Delta C_{p,i}$ are not used in the interpretation of the kinetic data.

Table 2: Comparison of the Thermodynamic Parameters of Unfolding of CspB at pH 7.0, 25 °C, As Obtained from the Analyses of the Folding Kinetics and of the Equilibrium Transitions[a]

	thermal unfolding[b]	kinetics[c]
ΔH_{H_2O} (kJ/mol)	58.4 ± 4.3	64.4 ± 4.0
ΔH_i [kJ/(mol·M)]	−0.2 ± 0.7	1.1 ± 1.6
ΔS_{H_2O} [J/(mol·K)]	166 ± 14	186 ± 13
ΔS_i [J/(mol·K·M)]	8.0 ± 2.5	13 ± 6
$\Delta C_{p,H_2O}$ [kJ/(mol·K)]	3.8 ± 0.3	3.0 ± 0.5
$\Delta C_{p,i}$ [J/(mol·K·M)]	24 ± 73	216 ± 152
ΔG_{H_2O} (kJ/mol)	8.9[d]	8.9[d]
ΔG_i [kJ/(mol·M)]	−2.60[d]	−2.77[d]

[a] The thermodynamic values refer to solvent conditions of 0.1 M sodium cacodylate/HCl pH 7.0. [b] Thermodynamic data from the analysis of the equilibrium transitions in Figure 5. [c] Difference of the activation parameters for unfolding and refolding; they are taken from Table 1. [d] Standard deviations are not given for ΔG_{H_2O} and ΔG_i because these parameters do not result from the fits to eqs 6 and 7.

The best coincidence between the kinetic and the equilibrium parameters is found in the range of 20−40 °C and 3−5 M urea, conditions under which both the kinetics and the thermal unfolding could be measured with highest precision. Together the comparisons in Figure 6 provide additional good evidence that both the folding kinetics and the equilibrium stability of CspB obey the two-state model in eq 1 and are well described by the thermodynamic activation parameters in Table 1. In particular, coincident

values for ΔC_p and ΔG_i (m) as derived from the equilibrium transitions and from the difference of the kinetic activation data are regarded as good criteria for a two-state folding reaction.

DISCUSSION

Activation Parameters for the Unfolding and Refolding of CspB. In a wide range of temperature and urea concentration both the equilibrium transitions and the folding kinetics of CspB are well described by a N ⇌ U two-state mechanism. Under all conditions folding was a reversible monoexponential reaction, and evidence for populated folding intermediates could neither be found at equilibrium, nor in the folding kinetics. The close adherence to the two-state mechanism encouraged us to use the transition state theory for analyzing the observed kinetics and to calculate the activation parameters for unfolding and refolding. The analysis gives the values for the activation enthalpy $\Delta H^{\ddagger}$ and the heat capacity of activation $\Delta C_p^{\ddagger}$. The activation entropies $\Delta S^{\ddagger}$ depend on the choice of the preexponential factor in the Eyring equation. In the transition state theory (Hänggi *et al.*, 1990) the transmission coefficient κ is set to 1, but for complex reactions, such as protein folding, its value is not known. The magnitude of $\Delta S^{\ddagger}$ depends on the logarithm of κ, and therefore only relative values can be calculated for $\Delta S^{\ddagger}$ from the kinetic data. The changes in $\Delta S^{\ddagger}$ with variables such as temperature or denaturant concentration may, however, be readily interpreted.

Location of the Transition State for Folding. In a two-state folding transition two thermodynamic criteria are most often used to locate the transition state with respect to the unfolded and the native state. The relative kinetic m values [defined as $\Delta G_i^{\ddagger}/\Delta G_i(\mathrm{eq})$] report on the interactions of the transition state with the solvent (Tanford, 1968; Matthews, 1993), and the relative values of the activation heat capacity [$\Delta C_p^{\ddagger}/\Delta C_p(\mathrm{eq})$] report on the hydrophobic and polar hydration of the protein in the transition state (Makhatadze & Privalov, 1994, 1995). In equilibrium protein denaturation the m and ΔC_p values correlate well with each other because both depend on the amount of protein surface which becomes exposed to solvent upon unfolding (Myers *et al.*, 1995; Makhatadze & Privalov, 1995). For the folding mechanism of CspB the changes in m and ΔC_p give the same clear answer. During refolding in the absence of urea 90% of the change in ΔC_p and 96% of the change in m occur between the unfolded and the activated state, i.e., the activated state is "more than 90% native" by these two criteria. This is reflected in the experimental data. The rate constant of unfolding is virtually independent of the urea concentration (Figure 2), and in the Arrhenius plot it shows an almost linear dependence on temperature (Figure 3) because the native and the activated state do not differ significantly in their interactions with urea and water.

To our knowledge the thermodynamic properties of the transition state of CspB are fairly unique. A similarly extensive kinetic investigation of both thermally and denaturant-induced unfolding, which does not rely on the input of equilibrium data, has rarely been carried out with other proteins. A transition state with a heat capacity as the native protein was found for the folding of hen lysozyme with intact disulfide bonds (Segawa & Sugihara, 1984); but by the m criterion this transition state is only about 70% native (Tanford, 1968; Kiefhaber, 1995). The transition state of the folding of T4 lysozyme is about 75% native as deduced by Chen *et al.* (1989, 1992) from an equilibrium and kinetic investigation of the cold denaturation of this protein, also by using the m and $\Delta C_p^{\ddagger}$ criteria. In the folding of chymotrypsin inhibitor 2 (CI2) the transition state was originally also assumed to be native-like, because $\Delta C_p^{\ddagger}(\mathrm{U}\rightarrow\mathrm{N})$ was found to be identical with $\Delta C_p(\mathrm{eq})$ (Jackson & Fersht, 1991b). Later, the same group determined a much smaller value for $\Delta C_p^{\ddagger}(\mathrm{U}\rightarrow\mathrm{N})$ for the folding of this protein (Oliveberg *et al.*, 1995), which would agree with the proposition that the transition state of CI2 is largely unfolded (Itzhaki *et al.*, 1995).

Thermodynamic Properties of the Refolding Reaction of CspB. The native-like character of the activated state has interesting consequences for the refolding reaction of CspB. The equilibrium stability of proteins is generally small and results from a pronounced compensation of enthalpy and entropy (Privalov, 1979). This compensation is strongly dependent on temperature, because, as a consequence of the changes in the hydration of the nonpolar residues, the heat capacity increases strongly during unfolding. Since the activated state of folding of CspB is so close to the native state, this temperature-dependent change in the enthalpy/entropy compensation is reflected in the activation parameters of refolding. This is clearly seen in Figure 4B,C. At 10 °C $\Delta H^{\ddagger}$ is positive and very large (75 kJ/mol), and $\Delta S^{\ddagger}$ is also positive [70 kJ/(K·mol)]. Thus the kinetics of refolding at low temperature strongly resemble the thermally induced equilibrium folding transitions of proteins at low temperature, which are always characterized by positive values for ΔH_{eq} and ΔS_{eq} (the signs refer to the *refolding* direction) (Makhatadze & Privalov, 1995).

$\Delta H^{\ddagger}$ and $\Delta S^{\ddagger}$ of refolding decrease strongly with temperature. At 37 °C both are already slightly negative (Figure 4B), indicating that the barrier to refolding becomes increasingly entropic with increasing temperature. At first glance, this might be expected for a folding reaction in which the reduction of the huge number of conformations of the unfolded state to a few productive activated states is the major barrier on the route to the native state (Bryngelson *et al.*, 1995). However, this simple interpretation of our results, which considers only the changes within the folding protein chain itself, is misleading, because the absolute values of $\Delta S^{\ddagger}$ are not known, and, more importantly, because the changes in the solvent are neglected. From the thermodynamic analyses of equilibrium protein folding it is now clear that these changes in the solvent and not the intra-protein interactions are responsible for the decrease in heat capacity during folding, and thus for the strong decrease with temperature of the enthalpy and the entropy of folding (Makhatadze & Privalov, 1994, 1995). Similarly, the decreases in the activation enthalpy and activation entropy of refolding are also caused by the differential solvation of the unfolded and the activated state of folding. Both the enthalpy and the entropy of desolvation of hydrophobic residues are very large at low temperature, but decrease strongly with increasing temperature (Makhatadze & Privalov, 1994, 1996). Thus, the entropy of hydration can compensate for the loss in the conformational entropy of the protein chain during folding at low temperature but not at high temperature.

This shows clearly that not the chain folding itself, but the changes in the solvent around the native-like activated state lead to the observed transition from an enthalpic to an entropic barrier. It is thus a consequence of the hydrophobic effect.

The activation parameters of unfolding of CspB do not change significantly with temperature and with urea concentration. $\Delta H^{\ddagger}$ shows a large positive value of about 100 kJ/mol under all conditions. This indicates that, although the transition state of folding has already native-like interactions with the solvent, it still differs significantly from the fully folded state in its enthalpy. Probably, a fraction of the native stabilizing interactions are not yet formed in the transition state.

Intermediates and Activated States in Protein Folding. Several simple proteins (without disulfide bonds or tightly bound cofactors) are now known which fold unusually fast. These proteins differ in three dimensional structure, but all of them are small, single-domain proteins or small fragments of larger proteins. Apart from ubiquitin (Khorasanizadeh *et al.*, 1996), they follow N ⇌ U two-state mechanisms both in their equilibrium transitions and in their folding kinetics. Thus it seems that rapid folding and the absence of populated intermediates are correlated with the small size of these proteins. Small proteins contain fewer stabilizing interactions than large ones, and, as a consequence, their cooperativities and stabilities are low. Folding intermediates which contain only a part of the native-like interactions are probably unstable and, once formed, they rapidly revert back to the unfolded state. This could explain, why a folding intermediate could be found only for ubiquitin (Khorasanizadeh *et al.*, 1996), which shows a higher stability than the other small proteins. The instability of the intermediates could provide an efficient means to avoid trapping in incorrect, partially-folded states and could thus contribute to the rapid folding.

The role of intermediates for protein folding is not clear (Baldwin, 1996; Fersht, 1995). In several of the current models for protein folding productive intermediates are assumed to be unstable to warrant the high cooperativity of the folding process, and the activated state is assumed to be native-like (Go, 1983; Creighton *et al.*, 1996; Privalov, 1996; Jonsson *et al.*, 1996). According to these models the activated state is reached when the cooperativity of the emerging folded structure has increased to the point where the probability of making additional interactions becomes higher than the probability of losing already existing interactions. As a logical consequence small proteins with few cooperative interactions should not show intermediates and reach their transition state in folding later than larger ones. This was pointed out recently also by Sosnick *et al.* (1996).

Of course, rapid folding along such a scheme (Creighton *et al.*, 1996) is only possible when the folding protein chain avoids misfolding *after* it has crossed the activation barrier. We suggest that the probability for "downhill" folding after the activation barrier is highest when the activated state shows already a strongly native structure.

However, a native-like activated state as in the folding of CspB is not observed for other small fast-folding proteins. The acyl-CoA binding protein (Kragelund *et al.*, 1995, 1996), the fragment of λ repressor (Huang & Oas, 1995), cytochrome *c* (Sosnick *et al.*, 1994, 1996), and the chymotrypsin inhibitor CI2 (Jackson & Fersht, 1991a,b) all show activated states which, by the *m* criterium are about 50% native-like. The first two proteins are predominantly α-helical and CI2 is a mixed α/β protein. In contrast, CspB contains only β-structure. It is possible that the extent of folded structure in the transition state correlates with the secondary structure of a protein. Unlike β-sheets, α-helices are local structures and therefore individual helices can form very easily and, in the transition state, serve as kernels for the rapid assembly of the remaining structure. Such a facile formation of local structure can of course also lead to non-native structures and thus decelerate overall folding.

In the light of these considerations the folding of CspB appears highly optimized. Its single β-sheet requires a major fraction of its cooperative interactions to stabilize it. Thus, all intermediates prior to the activated state are unstable, and the activated state is not reached until the protein is almost native. Thereafter, the well-ordered structure of the activated state efficiently prevents misfolding and guarantees that the native state is reached rapidly. Intriguingly, the activated state of folding of another small β-protein, the SH3 domain of spectrin (Viguera *et al.*, 1994), is also fairly native. Its *m* value for refolding amounts to about 80% of the equilibrium *m* value. Apparently, the inherent difficulty to form the β-sheet is not a disadvantage in the folding of CspB. Rather, alternative non-native structures are even less stable. Therefore they are avoided and productive folding is very fast and efficient.

ACKNOWLEDGMENT

We thank Peter Graumann and Mohamed Marahiel for a strain of *E. coli* which overproduces CspB and Vishwas Agashe, Jochen Balbach, Maik Jacob, and Stefan Walter for discussions of this work.

REFERENCES

Agashe, V. R., & Udgaonkar, J. B. (1995) *Biochemistry 34*, 3286−3299.
Baldwin, R. L. (1996) *Folding Des. 1*, R1−R8.
Bryngelson, J. D., Onuchic, J. N., Socci, N. D., & Wolynes, P. G. (1995) *Proteins: Struct., Funct., Genet. 21*, 167−195.
Chen, B. L., Baase, W. A., & Schellman, J. A. (1989) *Biochemistry 28*, 691−699.
Chen, B. L., Baase, W. A., Nicholson, H., & Schellman, J. A. (1992) *Biochemistry 31*, 1464−1476.
Chen, X. W., & Matthews, C. R. (1994) *Biochemistry 33*, 6356−6362.
Creighton, T. E., Darby, N. J., & Kemmink, J. (1996) *FASEB J. 10*, 110−118.
Fersht, A. R. (1995) *Proc. Natl. Acad. Sci. U.S.A. 92*, 10869−10873.
Go, N. (1983) *Annu. Rev. Biophys. Bioeng. 12*, 183−210.
Hänggi, P., Talkner, P., & Borkovec, M. (1990) *Rev. Modern Phys. 62*, 251−341.
Huang, G. S., & Oas, T. G. (1995) *Proc. Natl. Acad. Sci. U.S.A. 92*, 6878−6882.
Itzhaki, L. S., Otzen, D. E., & Fersht, A. R. (1995) *J. Mol. Biol. 254*, 260−288.
Jackson, S. E., & Fersht, A. R. (1991a) *Biochemistry 30*, 10428−10435.
Jackson, S. E., & Fersht, A. R. (1991b) *Biochemistry 30*, 10436−10443.
Jaenicke, R. (1987) *Prog. Biophys. Mol. Biol. 49*, 117−237.
Jaenicke, R. (1996) *Curr. Topics Cell. Reg. 34*, 209−314.
Jones, P. G., van Bogelen, R. A., & Neidhardt, F. C. (1987) *J. Bacteriol. 169*, 2092−2095.
Jonsson, T., Waldburger, C. D., & Sauer, R. T. (1996) *Biochemistry 35*, 4795−4802.
Khorasanizadeh, S., Peters, I. D., Butt, T. R., & Roder, H. (1993) *Biochemistry 32*, 7054−7063.

Khorasanizadeh, S., Peters, I. D., & Roder, H. (1996) *Nat. Struct. Biol. 3*, 193−205.
Kiefhaber, T. (1995) *Proc. Natl. Acad. Sci. U.S.A. 92*, 9029−9033.
Kragelund, B. B., Robinson, C. V., Knudsen, J., Dobson, C. M., & Poulsen, F. M. (1995) *Biochemistry 34*, 7217−7224.
Kragelund, B. B., Hojrup, P., Jensen, M. S., Schjerling, C. K., Juul, E., Knudsen, J., & Poulsen, F. M. (1996) *J. Mol. Biol. 256*, 187−200.
Kraulis, P. J. (1991) *J. Appl. Crystallogr. 24*, 946−950.
Lesk, A. M., & Rose, G. D. (1981) *Proc. Natl. Acad. Sci. U.S.A. 78*, 4304−4308.
Makhatadze, G. I., & Marahiel, M. A. (1994) *Protein Sci. 3*, 2144−2147.
Makhatadze, G. I., & Privalov, P. L. (1994) *Biophys. Chem. 51*, 291−309.
Makhatadze, G. I., & Privalov, P. L. (1995) *Adv. Protein Chem. 47*, 307−425.
Makhatadze, G. I., & Privalov, P. L. (1996) *Protein Sci. 5*, 507−510.
Matouschek, A., Kellis, J. T., Serrano, L., Bycroft, M., & Fersht, A. R. (1990) *Nature 346*, 440−445.
Matouschek, A., Otzen, D. E., Itzhaki, L. S., Jackson, S. E., & Fersht, A. R. (1995) *Biochemistry 34*, 13656−13662.
Matthews, C. R. (1993) *Annu. Rev. Biochem. 62*, 653−683.
Myers, J. K., Pace, C. N., & Scholtz, J. M. (1995) *Protein Sci. 4*, 2138−2148.
Oliveberg, M., Tan, Y.-J., & Fersht, A. R. (1995) *Proc. Nat. Acad. Sci. U.S.A. 92*, 8926−8929.
Pace, C. N. (1986) *Methods Enzymol. 131*, 266−280.
Privalov, P. L. (1979) *Adv. Protein Chem. 33*, 167−241.
Privalov, P. L. (1996) *J. Mol. Biol. 258*, 707−725.
Schellman, J. A. (1978) *Biopolymers 17*, 1305−1322.
Schindelin, H., Herrler, M., Willimsky, G., Marahiel, M. A., & Heinemann, U. (1992) *Proteins: Struct., Funct., Genet. 14*, 120−124.
Schindelin, H., Marahiel, M. A., & Heinemann, U. (1993) *Nature 364*, 164−168.
Schindler, T., Herrler, M., Marahiel, M. A., & Schmid, F. X. (1995) *Nat. Struct. Biol. 2*, 663−673.
Schnuchel, A., Wiltschek, R., Czisch, M., Herrler, M., Willimsky, G., Graumann, P., Marahiel, M. A., & Holak, T. A. (1993) *Nature 364*, 169−171.
Segawa, S.-I., & Sugihara, M. (1984) *Biopolymers 23*, 2473−2488.
Sosnick, T. R., Mayne, L., Hiller, R., & Englander, S. W. (1994) *Nat. Struct. Biol. 1*, 149−156.
Sosnick, T. R., Mayne, L., & Englander, S. W. (1996) *Proteins: Struct., Funct., Genet. 24*, 413−426.
Tanford, C. (1968) *Adv. Protein Chem. 23*, 218−282.
Tonomura, B., Nakatani, H., Ohnishi, M., Yamaguchi-Ito, J., & Hiromi, K. (1978) *Anal. Biochem. 84*, 370−383.
Viguera, A. R., Martinez, J. C., Filimonov, V. V., Mateo, P. L., & Serrano, L. (1994) *Biochemistry 32*, 2142−2150.
Wetlaufer, D. B., & Ristow, S. (1973) *Annu. Rev. Biochem. 42*, 135−158.
Willimsky, G., Bang, H., Fischer, G., & Marahiel, M. A. (1992) *J. Bacteriol. 174*, 6326−6335.

BI962090J